Earth and Planetary Science Letters xxx (2008) xxx–xxx

Contents lists available at ScienceDirect

Earth and Planetary Science Letters

journal homepage: www.elsevier.com/locate/epsl

The snowball Earth aftermath: Exploring the limits of continental weathering processes

Guillaume Le Hir [a], Yannick Donnadieu [a], Yves Goddéris [b,*], Raymond T. Pierrehumbert [c], Galen P. Halverson [d], Mélina Macouin [b], Anne Nédélec [b], Gilles Ramstein [a]

[a] LSCE, CNRS-CEA-UVSQ, Gif-sur-Yvette, France
[b] LMTG, CNRS-Université de Toulouse, Observatoire Midi-Pyrénées, Toulouse, France
[c] Dept of Geophysical Sciences, University of Chicago, Illinois, USA
[d] School of Earth and Environmental Sciences, University of Adelaide, North Terrace, Adelaide, SA 5005, Australia

ARTICLE INFO

Article history:
Received 22 May 2008
Received in revised form 10 October 2008
Accepted 10 November 2008
Available online xxxx

Editor: P. DeMenocal

Keywords:
snowball Earth
greenhouse
cap dolostones
weathering
modelling

ABSTRACT

Carbonates capping Neoproterozoic glacial deposits contain peculiar sedimentological features and geochemical anomalies ascribed to extraordinary environmental conditions in the snowball Earth aftermath. It is commonly assumed that post-snowball climate dominated by CO_2 partial pressures several hundred times greater than modern levels, would be characterized by extreme temperatures, a vigorous hydrological cycle, and associated high continental weathering rates. However, the climate in the aftermath of a global glaciation has never been rigorously modelled. Here, we use a hierarchy of numerical models, from an atmospheric general circulation model to a mechanistic model describing continental weathering processes, to explore characteristics of the Earth system during the supergreenhouse climate following a snowball glaciation. These models suggest that the hydrological cycle intensifies only moderately in response to the elevated greenhouse. Indeed, constraints imposed by the surface energy budget sharply limit global mean evaporation once the temperature has warmed sufficiently that the evaporation approaches the total absorbed solar radiation. Even at 400 times the present day pressure of atmospheric CO_2, continental runoff is only 1.2 times the modern runoff. Under these conditions and accounting for the grinding of the continental surface by the ice sheet during the snowball event, the simulated maximum discharge of dissolved elements from continental weathering into the ocean is approximately 10 times greater than the modern flux. Consequently, it takes millions of years for the silicate weathering cycle to reduce post-snowball CO_2 levels to background Neoproterozoic levels. Regarding the origin of the cap dolostones, we show that continental weathering alone does not supply enough cations during the snowball melting phase to account for their observed volume.

1. Introduction

Geological evidence suggests the occurrence of two global glaciations during the Neoproterozoic. The older glaciation, the Sturtian event, is commonly inferred to have occurred at ca. 700–680 Ma, while the latter, end-Cryogenian glaciation ended at 635 Ma (Hoffman et al., 2004; Condon et al., 2005). The melting of these snowball Earth events requires very high atmospheric pCO_2, so that the greenhouse warming overcomes the freezing feedback induced by a high sea-ice albedo. The amount of CO_2 required to initiate melting of a snowball was first calculated to be 0.12 bar (400 PAL) using a simple energy balance model (Caldeira and Kasting, 1992) but more recent modelling suggests it was above 0.2 bar (660 PAL) (Pierrehumbert, 2004). Geochemical evidence seems to confirm exceptionally high pCO_2 following at least the 635 Ma snowball event (Kaseman et al., 2005; Bao et al., 2008), but the behavior of this supergreenhouse climate under very high CO_2 levels is still poorly understood. Was it just a short pulse, lasting a few hundreds of kyrs, or was it longer-lived, with environmental consequences enduring for millions of years? According to the classic snowball Earth hypothesis the supergreenhouse drove a hyper-active hydrological cycle inducing intense continental weathering, such that CO_2 levels would have been drawn down from very high levels to preglacial levels in about 200 kyrs (Higgins and Schrag, 2003).

Up to now, this timespan subsequent to the snowball glacial event has never been investigated with a comprehensive climate model. In this contribution, four numerical models (Fig. 1) are used to investigate the evolution of the post glacial climate: (1) a 3D-climate model to characterize the super hothouse climate, (2) a continental weathering model to investigate the behaviour of the CO_2 weathering sink, (3) a simple carbon-alkalinity cycle model to simulate the evolution of the atmospheric CO_2 levels in the immediate aftermath of the snowball Earth, and (4) a simple eustatic model to investigate the

* Corresponding author.
E-mail address: godderis@lmtg.obs-mip.fr (Y. Goddéris).

0012-821X/$ – see front matter © 2008 Elsevier B.V. All rights reserved.
doi:10.1016/j.epsl.2008.11.010

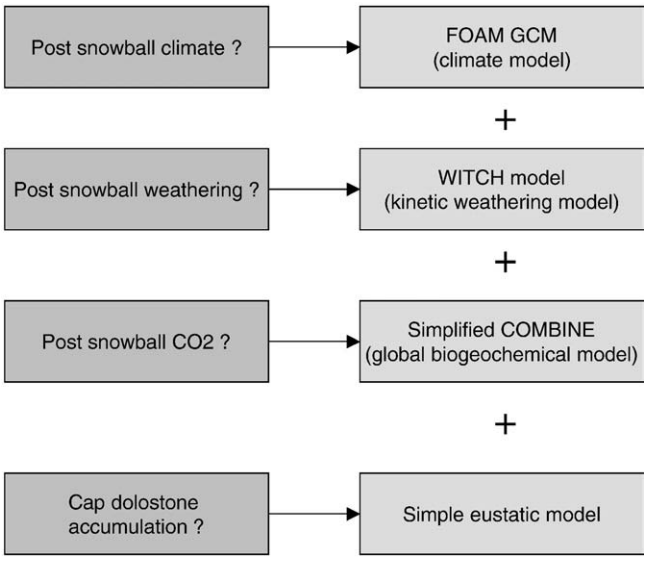

Fig. 1. General design of the simulations. At each level, a question is added and addressed using a specific model. When going down through the diagram, any new specific question requires the coupling of a hierarchy of models (specified by the sign '+').

consequences of post snowball continental weathering on cap dolostone accumulation. Our aim is to use numerical modelling to produce a first order reconstruction of the supergreenhouse climate and the timescale over which it is relaxed. Weathering processes are influenced by the air temperature controlling the dissolution rates of minerals, and by the continental runoff, which modulates dissolution through water-rock interactions and carries the weathering products to the oceans. We will first focus on climatic reconstructions of the supergreenhouse environment, after which the behaviour of the weathering sink under this climate will be discussed, and its consequences on the duration of the supergreenhouse will be investigated. Specifically, we will address the accumulation of cap dolostones which were deposited during the post glacial eustatic transgression and are a key element of the snowball hypothesis.

2. The climate of the snowball aftermath

2.1. Climate model description and simulation design

The climate of the post snowball is investigated with the general circulation climate model FOAM 1.5. The atmospheric component of FOAM is a parallelized version of NCAR's Community Climate Model 2 (CCM2) with the upgraded radiative and hydrologic physics incorporated in CCM3 v. 3.2 (Jacob, 1997). All simulations have been performed with an R15 spectral resolution (4.5°×7.5°) and 18 vertical levels. FOAM is used in mixed-layer mode, meaning the atmospheric model is linked to a 50-meter mixed-layer ocean with heat transport parameterized through diffusion. FOAM has been extensively applied to the study of ancient climate (Poulsen, 2003; Poulsen and Jacob, 2004; Donnadieu et al., 2006) and Pierrehumbert has demonstrated the validity of the FOAM radiative code in highly enriched CO_2 atmospheres such as the one hypothesized in the snowball Earth aftermath (Pierrehumbert, 2004). We have used a simplified paleogeographic model for the late Cryogenian (i.e. Marinoan) adapted from Macouin [pers.com] wherein the continental fragments of the former supercontinent Rodinia are clustered in low latitudes. An orography is assumed considering geological features (old orogenic belts and recent rifting) (Meert and Torsvik, 2003) [Macouin, pers. com.] (Fig. 2). We prescribe the presence of orogens and rifts (Meert and Torsvik, 2003) as elevated areas, between 500 and 1100 m (these relatively low altitudes are the consequence of the spectral smoothing implied by the model low surficial resolution), while the continental area outside uplifted surface has an elevation of 75 m. Solar luminosity is fixed at 94% of its present day value (1286 W/m^2) according to stellar evolution models (Gough, 1981). Orbital parameters are set at their present day values. Regarding continental runoff, a present day simulation of FOAM linked to the mixed-layer ocean predict a global value of 27 cm/yr, a value very close to the observed 25 cm/yr (Berner and Berner, 1987) or 22 cm/yr (Gaillardet et al., 1999).

The melting phase of the snowball Earth has never been investigated. Indeed, modelling the climate under several hundred times the present day CO_2 pressure and with the presence of melting icecaps but also of melting sea-ice glaciers remains an unsolved challenge in terms of numerical tools and of computational times. The aim of this paper is not to model in detail the deglaciation: rather the

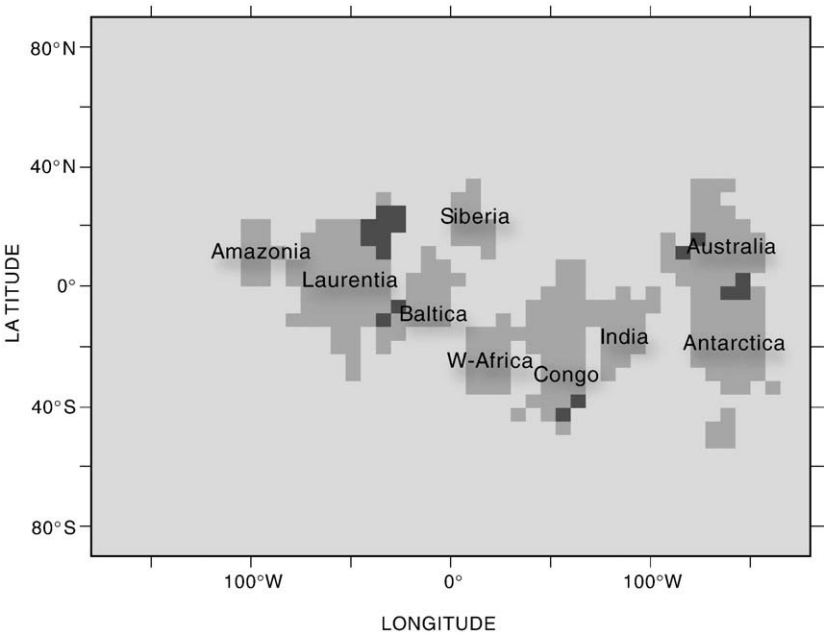

Fig. 2. End-Cryogenian (ca. 635 Ma) paleogeography used in the numerical modelling in this paper. Location of continental flood basalt provinces are shown in dark grey.

Please cite this article as: Le Hir, G., et al., The snowball Earth aftermath: Exploring the limits of continental weathering processes, Earth Planet. Sci. Lett. (2008), doi:10.1016/j.epsl.2008.11.010

focus here is on the supergreenhouse climate occurring just after the melting of the continental and sea ice. Considering the Neoproterozoic solar weakness and nonlinear relation between CO_2 concentration and the resultant greenhouse forcing, the following range of atmospheric CO_2 mixing ratios (400, 200, 100, 50, 25, 20, 15, and 10 PAL) has been used to model the influence of CO_2 concentrations on post-glacial temperature and runoff. The simulations reach equilibrium with the prescribed boundary conditions after 30 years. The analyses are done using the average of the next ten years. All the continents are assumed to be covered with a rocky regolith (visible albedo 0.24, infrared albedo 0.4, roughness 0.05 m, potential evaporation 0.1)

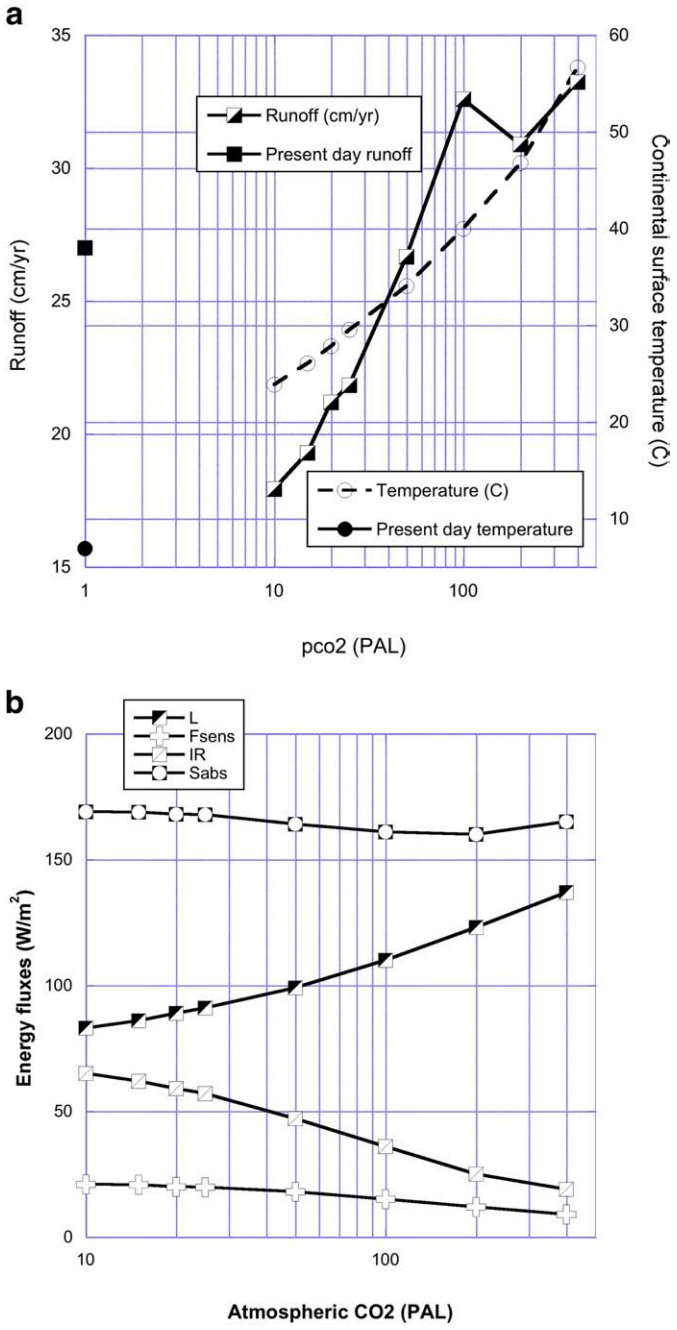

Fig. 3. a) Mean continental runoff and mean continental temperature calculated by the FOAM GCM under Neoproterozoic conditions and for various atmospheric CO_2 levels. The calculated present day values are also shown b) Energy fluxes calculated by the FOAM GCM under Neoproterozoic conditions and for various atmospheric CO_2 levels. *L* is the latent heat, F_{sens} the sensible heat, IR the surface infra-red cooling and S_{abs} the total incoming solar radiation adsorbed by the surface.

Table 1
Water vapor mixing ratio at 5 different CO_2 levels for Neoproterozoic conditions, 1 PAL equals 280 ppm

Atmospheric pCO_2 (PAL)	q_s	q	P (mm/mo)	Land ratio
400	0.064	0.052	141	0.88
200	0.042	0.035	127	0.96
100	0.029	0.024	113	0.94
50	0.022	0.018	102	0.88
10	0.014	0.011	85	0.825

q_s is the saturation water vapor mixing ratio at surface air temperature, in kg water per kg air. q is the actual water mixing ratio of the air, in kg water per kg air. P is the global mean precipitation in mm/month, and the "land ratio" is the ratio of the mean precipitation rate over land to the global mean precipitation rate.

2.2. Post snowball Earth climate: runoff and water cycle behaviour

Fig. 3a shows average terrestrial temperature and runoff evolution as a function of the atmospheric CO_2 mixing ratio. The mean continental temperature exhibits a roughly logarithmic response to CO_2 rise while runoff follows two pathways in our runs, a first one characterized by a logarithmic increase and a second one, above 100 PAL, characterized by a runoff saturating around 30–33 cm/yr which corresponds to a maximum increase of 22% when compared to the simulated runoff under present-day climate. This modest increase in runoff despite vastly higher pCO_2 sharply contrasts with the 7 fold increase in runoff assumed in the only other attempt to model silicate weathering rates under a post-snowball climate. In this previous study (Kump pers. com. in Higgins and Schrag, 2003), maximum runoff increase was estimated based on the inventory of the maximum amplitude of a variety of hydrological factors (Holland, 1978). As will be discussed further in Section 3, our result has important consequences for the rates of chemical weathering and geochemical evolution of the oceans following a snowball glaciation.

The weak increase in precipitation (and hence in runoff) with temperature in the post-Snowball world plays a key role in our results, and so merits some further discussion. In fact, a very similar phenomenon, although smaller, has attracted a lot of attention with regard to the effect of anthropogenic global warming on precipitation (notably Held and Soden, 2006). In particular, it has been found in virtually all climate simulations that increasing temperature by doubling or quadrupling CO_2 increases the precipitation much less than one would expect from the increase in saturation vapor pressure obtained from the Clausius-Clapeyron relation. Specifically, the Clausius-Clapeyron relation predicts that precipitation should increase by about 7% per degree of warming, whereas the actual figure for moderate warming is more like 2%. The presumed explanation for this disparity is that as the planet warms, atmospheric circulation becomes more sluggish, so that even though there is more water in the system, the rate at which it condenses into rain does not increase much (Vecchi et al., 2006). Atmospheric circulation weakens with the increase of atmospheric CO_2 levels in our simulations, in particular, the mean annual stream function zonally averaged is divided by 5 between the 20 PAL and the 400 PAL runs (figure not shown).

It has often been thought that infrared radiative cooling places an *a priori* constraint on precipitation, given that the dominant energy balance in the atmosphere is between latent heat release and radiative cooling (see Allen and Ingram, 2002 for a recent review of such arguments). However, Pierrehumbert (Pierrehumbert, 1999) showed that the argument is fallacious, or at least incomplete, since in principle the surface conditions can adjust to allow whatever column-integrated infrared cooling is necessary to accommodate the evaporation required to sustain a given precipitation level. In order to understand constraints on precipitation, a detailed consideration of the surface energy budget is unavoidable. In particular, it was argued

Please cite this article as: Le Hir, G., et al., The snowball Earth aftermath: Exploring the limits of continental weathering processes, Earth Planet. Sci. Lett. (2008), doi:10.1016/j.epsl.2008.11.010

that the evaporation from the surface is in effect limited by the supply of solar radiation absorbed at the surface, so that if one warms the climate by increasing CO_2 without changing the solar radiation, there comes a threshold above which all solar radiation is used to sustain evaporation, whereafter precipitation no longer increases with temperature. This argument was extended and made more quantitative in Pierrehumbert (2002), where it was pointed out that the evaporation can somewhat exceed the solar absorption, but that the excess tends to be limited by the properties of turbulent fluxes in a stable boundary layer. This limitation in the increase in precipitation rates with increased pCO_2 has important implications for silicate weathering, and it is these implications that we explore in the Snowball recovery simulations here.

Table 1 and Fig. 3b summarize key boundary layer and surface budget properties pertinent to the hydrological cycle. As CO_2 is increased from 10 PAL to 400 PAL, the low level saturation mixing ratio increases by a factor of 4.6, and the actual boundary layer mixing ratio increases by a similar factor. However, the global precipitation rate only increases by 60%, with a proportional increase over the continents. To understand this relationship, it is necessary to examine the components of the surface energy budget. The following equation describes the global energy budget of the Earth surface:

$$S_{abs} = L + F_{sens} + IR. \quad (1)$$

where S_{abs} is the global solar radiation absorbed by the surface, L is the latent heat flux (evaporation), F_{sens} is the sensible heat flux and IR the net infrared cooling of the surface. The mass flux of water due to evaporation is proportional to L, which hence determines the global precipitation rate. The net infrared cooling rate of the surface is the upward flux $\sigma T^4_{surface}$ minus the infrared back-radiation from the atmosphere. To the extent that F_{sens} and IR balance some of the incoming solar absorption, they capture energy that would otherwise be used to sustain evaporation. Both F_{sens} and IR increase as the surface is made increasingly warmer than the overlying atmosphere; they tend to be small when the air and surface temperatures are close, and moreover as the temperature increases and the boundary layer becomes more moist the net infrared cooling falls to zero because the atmosphere radiates to the ground at the same temperature as the ground radiates to the atmosphere. Looking at the calculated energy budget in the Fig. 3b, we see that the solar absorption remains nearly constant as CO_2 is increased, but that the sensible and infrared cooling falls precipitously as the climate is made warmer. The slack is taken up by evaporation, but the total "extra" energy in the 10 PAL case is only 86 W/m^2. Indeed, we see that by the time we reach the 400 PAL case, evaporation balances 82% of the surface absorbed solar radiation.

Thus, the limited increase in runoff in these simulations is seen as a robust consequence of the behavior of the surface energy budget. Nevertheless, it should be reminded that the runoff depends also on how available water vapor is redistributed between land and ocean. In our particular case where most of the continents are located in the tropical regions, deep atmospheric convection as well as sea surface temperature distribution should be two major factors controlling the water transport between the ocean and the continent. While we are confident in the way FOAM simulates the former one, the latter one may suffer from uncertainties owing to the use of the mixed-layer version of the FOAM model. Nevertheless, although we acknowledge that the mixed-layer model may bias our results, we suspect that the global energetic arguments developed in the paper remain the first order process controlling the absolute value of the global runoff. The use of a fully coupled climate model is warranted in order to provide a definitive answer. Potential shortcomings of our results may also come from the cloud parameterizations and its behaviour in a very different climate than the modern one. One of the primary determinants of cloud forcing is the cloud water content. The FOAM cloud water parameterization and its limitations were described in Pierrehumbert (2004). In particular, while the scale height of cloud water increases in a warming climate, allowing high clouds to become more optically thick in a warmer world, the base-level cloud water parameter is independent on temperature. Insofar as there is more supply of water vapor in a hotter world, it is not unreasonable to expect that clouds at all levels might have higher water vapor content. In that case, the present simulations may underestimate the cloud water content. To test the implications of this possibility, we performed another run with 400× present CO_2, but with the cloud water parameter increased by a factor of 2. As a test in this run, both the cloud albedo effect and the cloud greenhouse effect roughly doubled compared to the control case, but the net cloud forcing remained nearly the same, with a slight shift toward more net cooling in the subtropics and more warming at the poles. The higher albedo did, however, reduce the surface absorbed solar radiation from 167 W/m^2 in the 400 PAL control case to 150 W/m^2 in the thick-cloud case. In accordance, this also reduced the global mean precipitation rate from 141 mm/mo to 114 mm/mo. Thus, higher cloud water content further reduces the precipitation. Nevertheless, the factors governing cloud fraction are poorly understood. In particular, there is observational evidence that for warm rain processes, cloud fraction goes down with temperature, owing to increased precipitation efficiency (Rapp et al., 2005). This feedback is not present in the cloud fraction scheme we are using. This is a fruitful area for future inquiry.

3. Continental weathering during the supergreenhouse climate

We now consider the weathering pattern as a function of the simulated climate. As shown in Section 2, the simulated post-glacial period is warm and moderately humid, with maximum continental runoff limited at 33 cm/yr above 100 PAL CO_2. Depending on this climate regime, the silicate weathering acts as a restoring force of the carbon cycle that reduces atmospheric CO_2. Continental weathering is a function of climate, increasing with temperature and continental runoff as demonstrated by numerous field studies (Brady, 1991; White and Blum, 1995; Dessert et al., 2001; Oliva et al., 2003). Based on the compilation of the main cation fluxes exported by small basaltic and granitic catchments, Dessert et al. (2001) and Oliva et al. (2003) have proposed parametric relationships linking the climatic parameters (mean annual temperature and runoff) to CO_2 consumption by the dissolution of silicate minerals. These laws are strictly valid only for the present day environment and do not include a direct dependence of rock weathering on the acidity of rainwater (Oliva et al., 2003). Exporting these laws into the post-snowball environment is tricky for three reasons: (1) The climate is exotic and is beyond the validity field of the parametric laws. (2) The Earth surface might have been largely modified by the global glaciation. That is, dynamic glaciation persisting for several millions of years might have produced fine grained materials (i.e. rock flour) with very high reactive surface areas, promoting the dissolution of minerals and the atmospheric CO_2 consumption. (3) The very high levels of atmospheric CO_2 in the snowball Earth aftermath (100–400 PAL) would have acidified the rainfall. These CO_2 levels, which are potentially above the common soil CO_2 levels encountered today, have promoted the mineral dissolution rates. Because the use of parametric laws to describe continental weathering cannot account for these three major changes, it is necessary to investigate the runoff-temperature-weathering feedback with a mechanistic model of silicate rock weathering in natural environments.

3.1. Description of the continental weathering model

Here we utilize the WITCH weathering model (Goddéris et al., 2006), which was initially developed to simulate weathering processes in soil profiles and in river catchments above silicate bedrock and calibrated on a granitic watershed. It successfully

Please cite this article as: Le Hir, G., et al., The snowball Earth aftermath: Exploring the limits of continental weathering processes, Earth Planet. Sci. Lett. (2008), doi:10.1016/j.epsl.2008.11.010

describes the seasonal evolution of the chemical composition of soil solutions as a function of water-rock-biosphere interactions, as well as the mean annual chemical composition of the main stream. For present day studies, WITCH is coupled to a biospheric model that calculates the water circulation in the soil, the partial pressure of CO_2 below ground level as a result of root respiration and organic carbon decay, and the uptake and release of cations by the living and dead biomass. WITCH calculates the dissolution of minerals as a function of the soil solution composition at each time step through kinetic laws derived from transition state theory concept (Eyring, 1935). The kinetic and thermodynamic parameters have been experimentally determined. Four dissolving species are accounted for (H^+, OH^-, H_2O and organic ligands, but hereafter the organic ligands dissolution will be neglected due to absence of terrestrial vegetation). The dissolution rate of a given mineral R_s is thus equals to:

$$R_s = A \cdot S_w \cdot \left[\sum_i k_i \exp\left(\frac{-E_a^i}{RT}\right) \cdot a_i^{n_i} \cdot f_{inh}\right](1-\Omega^s) \quad (2)$$

where A stands for the mineral reactive surface (m^2/m^3 of soil), S_w is the soil moisture saturation (function of the water volumetric content, Sverdrup and Warfinge, 1995), k_i and E_a^i are the dissolution rate constant and the activation energy for the i species-promoted dissolution, a_i and n_i stand for the activity of species i and the order of reaction with respect to the dissolving species i, respectively. f_{inh} describes the inhibiting effect of aqueous species on mineral dissolution (Oelkers et al., 1994; Schott and Oelkers, 1995; Devidal et al., 1997). Finally, the effect of departure from equilibrium on mineral dissolution/precipitation rates is accounted for by the factor $(1-\Omega^s)$, where Ω stands for the solution saturation index with respect to the particular solid and s is a stoichiometric number.

The WITCH model includes 32 silicate minerals. The number of soil layers that are modelled can be adapted to any specific problem. The mineral reactive surface is calculated according to a simple parametric law assumed to be an approximation of the solid BET surface (Brunauer et al., 1938; Sverdrup and Warfinge, 1995):

$$A = \left(8.0x_{clay} + 2.2x_{silt} + 0.3x_{sand} + 0x_{coarse}\right) \cdot \rho \quad (3)$$

where x_{clay}, x_{silt}, x_{sand} and x_{coarse} represent the textural fractions of the clay, silt, sand and coarse materials in the soil, such that $x_{clay}+x_{silt}+x_{sand}+x_{coarse}=1$. ρ is the soil density in g/m^3. We also include continental calcite and dolomite dissolution in the WITCH model. Because carbonate dissolution is several orders of magnitude faster than silicate dissolution, we assume that continental waters are at equilibrium respectively with the carbonate phases when their abundance exceeds 2% by volume of the bedrock (thus when carbonate rock is the dominant phase, geochemically speaking), and with the CO_2 partial pressure below ground level. The solubility product of dolomite is calculated as a function of the air temperature T (Drever, 1997):

$$K_{dol} = 10^{-17.09} \exp\left[-\frac{39480}{R} \cdot \left(\frac{1}{298.15} - \frac{1}{T}\right)\right] \quad (4)$$

where the standard enthalpy of reaction is in J/mol and R is the perfect gas constant.

For calcite, the solubility product is given by Drever (1997):

$$K_{cal} = 10^{-8.48} \exp\left[-\frac{9610}{R} \cdot \left(\frac{1}{298.15} - \frac{1}{T}\right)\right] \quad (5)$$

3.2. Design of the WITCH simulations

A number of parameters have to be fixed for using the WITCH model in the Neoproterozoic context. (1) The dissolution of minerals by organic ligands, and exchanges of elements with the living and dead biomass are set to zero because of the absence of continental vegetation at this time. (2) Since we aim at constraining the maximum CO_2 consumption in the post snowball environment, we assume granitic lithology covering all continental surface except where the occurrence of basaltic outcrops can be reasonably inferred from geological data (see compilation by Goddéris et al., 2003 and Fig. 2). Mineralogy of the granite and basalt used in WITCH are shown on Table 2. Carbonate weathering does not consume CO_2 on a 10^5 to 10^6 year timescale. Its role during the melting phase will be discussed in Section 5 (3) The volumetric content of water in the weathering profile has to be fixed. This parameter is important as it defines the fraction of the total reactive mineral surface that is wet and weatherable. In a first step, we fix it to a standard value of 0.2 m^3 water/m^3 soil. In a second step, we use the soil water content simulated by FOAM. (4) Given the assumed absence of soil biomass, CO_2 level is fixed in pore spaces to the atmospheric concentration. The WITCH model does not include a carbon budget of the below ground solutions so far. This means that the model is providing unlimited CO_2 to the water solutions, resulting in a possible slight overestimation of the weathering rates. (5) Assumptions about the thickness of the weathering profile and its texture are required in the model. We have chosen a shallow two layer structure with a thickness of 25 cm for the surface layer and of 100 cm for the deepest one. These relatively shallow thicknesses have been chosen based on the influence of persistent mechanical weathering during glaciation (Donnadieu et al., 2003), which would not allow the survival of any pre-glacial thick soil profiles. The soil system is assumed to have been largely reset by the glacial event. A sensitivity test to soil thickness is performed below. (6) With regards to the grain size, three tests have been run in which the reactive surface is changed according to Eq. (3) and intended to span the range of materials observed on the present earth surface. (7) temperature of the weathering profiles is taken from the GCM output field for the various atmospheric CO_2, and the GCM runoff is assumed to be equal to the vertical drainage of the weathering profile for each continental grid element. This assumption is valid because of the large size of the continental pixels in this study: all the water flowing through the weathering profiles can be assume to end up in a river draining the pixel.

3.3. Weathering rates in a supergreenhouse environment

Under 400 PAL, calculated CO_2 consumption by silicate weathering (Fig. 4a and b) ranges from 2.4 to 28 times the present-day flux, as estimated by Gaillardet et al. (1999), with the lowest value calculated assuming a coarse grain size (sand) material with reactive surface of 0.5×10^6 m^2/m^3 (LR run, Table 3). While such a coarse-grained surface layer on the continents is unlikely due to grinding by glaciers, this test provides a useful absolutely minimum level of silicate weathering to be expected. To test the sensitivity of weathering rates as a function of the mineral reactive surface, a finer grain size is used (MR run, Table 3), which yields a 6-fold increase over present day CO_2 consumption (Fig. 5a), showing that the mineral reactive surface is a crucial factor governing the post glacial weathering. In order to represent the Earth surface resulting from a global ice cover more precisely, we apply the reactive surface value measured on loesses derived from glacial erosion during the Last Glacial Maximum (Kahle et al., 2002) (13×10^6 m^2/m^3, HR run, Table 3) to the full 1.25 m-thick soil profile. In this run, which yields what we regard as a maximum value for weathering rates, the CO_2 consumption rate is 10 times

Table 2
Standard mineralogy for the silicated lithologies (in percent)

Granite	Quartz 31%	Orthose 26.5%	Andesine 42%	Apatite 0.3%
Basalt	Labradorite 45%	Basaltic glass 17.7%	Diopside 34%	Forsterite 2% Apatite 1.3%

Please cite this article as: Le Hir, G., et al., The snowball Earth aftermath: Exploring the limits of continental weathering processes, Earth Planet. Sci. Lett. (2008), doi:10.1016/j.epsl.2008.11.010

greater than the present-day value (Fig. 4a). A second run on a 6 m thick loess layer over the whole continental surface (Fig. 4a, run HR/thick) results in an increase in the calculated CO_2 consumption by a factor of only 2 to 3, which shows that predicted weathering rates are a non-linear function of loess thickness. This relationship is due to the limitation in weathering rates by the increase in the saturation state of pore water with respect to the primary silicate minerals as it percolates through the soil horizon. The result is significant because continental runoff is not commensurate with increased CO_2 levels, meaning soil waters rapidly reach oversaturation with respect to primary minerals.

Predicted CO_2 consumption by silicate weathering at low CO_2 levels (10 PAL) are all at least an order of magnitude below the present value of 11.7×10^{12} mol CO_2/yr (Gaillardet et al., 1999). These low predicted values are mainly driven by (1) the low below ground CO_2 levels (fixed at 10 PAL, which can be regarded as a lower hand value for

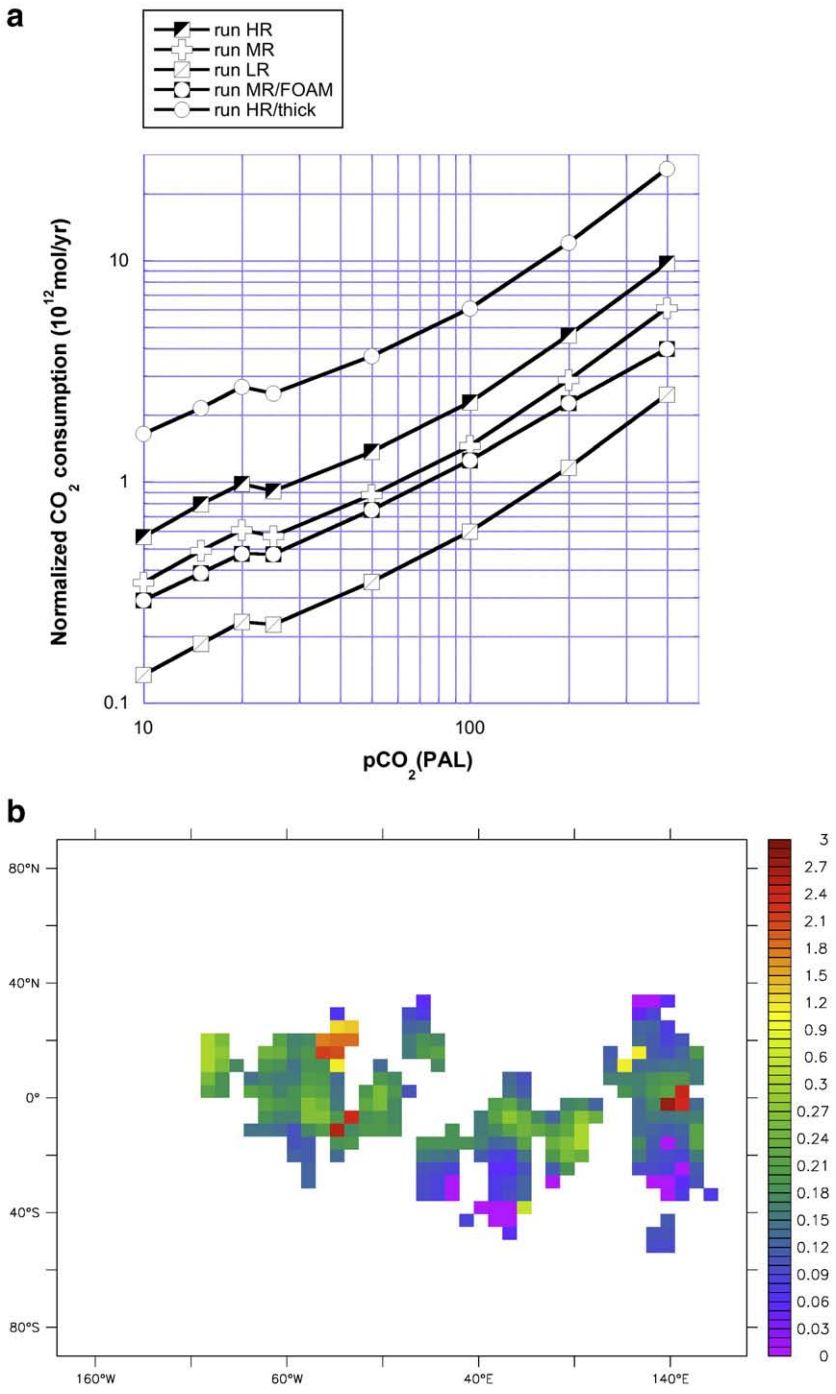

Fig. 4. a) Total CO_2 consumption by continental silicate weathering at various pCO_2 levels normalized to the present day value, as calculated by the WITCH model forced with the climatic output of the FOAM GCM. HR: high reactivity experiment, MR: middle reactivity experiment, LR: low reactivity experiment, HR/thick: high reactivity experiment with a 6 m-thick loess, and MR/FOAM: middle reactivity experiment with the water volumetric content of the loess calculated by FOAM. b) Calculated pattern of the CO_2 consumption by continental silicate weathering. at 400 PAL by the WITCH model(MR simulation, in 10^{12} mol/yr). Basaltic outcrop are identified by a higher flux.

Please cite this article as: Le Hir, G., et al., The snowball Earth aftermath: Exploring the limits of continental weathering processes, Earth Planet. Sci. Lett. (2008), doi:10.1016/j.epsl.2008.11.010

Table 3
WITCH simulations

WITCH simulation set	Temperature and runoff	Loess reactive surface (upper layer)	Water volumetric content of the loess
HR	FOAM	13×10^6 m^2/m^3	20%
MR	FOAM	6.2×10^6 m^2/m^3	20%
LR	FOAM	0.51×10^6 m^2/m^3	20%
MR/FOAM	FOAM	6.2×10^6 m^2/m^3	FOAM

All sets of run are using the FOAM climatology. Reactive surface of the upper layer (0.25 m thick) for the MR run (LR run) is calculated according to Eq. (3), assuming a grain size distribution with 25% clay and 75% silt materials (50% sandy and 50% coarse materials). Reactive surface of the upper layer for the HR run is prescribed at 13×10^6 m^2/m^3 based on Ref. The lower layer (1 m thick) contains sandy (50%) and coarse (50%) materials in all runs (yielding a reactive surface of 0.51×10^6 m^2/m^3), except for the HR run where we assumed a mineral reactive surface of the lower layer of 1×10^6 m^2/m^3.

present day soils), (2) the absence of organic acid produced by the biotic activity, (3) the relative aridity of the continental surfaces, (4) the smaller total continental surfaces (100×10^6 km^2 in the Neoproterozoic, compared to the 150×10^6 km^2 today).

4. Duration of the post-snowball supergreenhouse climate

Because the increase in CO_2 consumption by silicate weathering does not scale linearly with higher CO_2 levels, the post-snowball supergreenhouse climate should last much longer than the few hundred thousands years envisaged in the original snowball Earth model (Higgins and Schrag, 2003; Hoffman et al., 1998). Indeed, long term atmospheric CO_2 evolution is controlled by the balance between the solid Earth degassing and the total silicate weathering (Walker et al., 1981; Berner, 2004). No clear consensus exists concerning changes in the CO_2 outgassing flux in the geological past (Gaffin, 1987; Rowley, 2002; Cogné and Humler, 2004); thus we conservatively assume that the total solid earth degassing rate during the late Neoproterozoic was close to its present day value. Modelling the evolution of atmospheric CO_2 through geological times during a timespan where silicate weathering largely exceeds solid Earth degassing requires at least the calculation of the alkalinity and carbon budget of the surficial reservoirs (ocean+atmosphere), as well as the carbonate speciation in seawater. To perform these calculations, we use a simplified version of the COMBINE model (Goddéris and Joachimski, 2004), a box model with two oceanic reservoirs (surface and deep) and one for the atmosphere that has previously been applied to simulating the geochemical evolution of the snowball ocean (Le Hir et al., 2008a,b). CO_2 consumption by silicate weathering is taken from the FOAM/WITCH simulations, as a function of atmospheric CO_2. Since the WITCH model only gives cation and CO_2 consumption fluxes for the 8 solved climate scenarios (at 400, 200, 100, 50, 25, 20, 15 and 10 PAL CO_2), a linear interpolation for each continental grid cell (Fig. 2) is performed to define a continuous trend for cation fluxes as a function of atmospheric CO_2 between 400 and 10 PAL. Through this interpolation, we start from the CO_2 consumption fluxes calculated for each continental grid cell by the WITCH model, depending on the FOAM temperature and runoff, and end up with a simple trend describing the global CO_2 consumption through silicate rock weathering as a function of atmospheric CO_2. This interpolated flux is then incorporated at each timestep into the simplified COMBINE numerical model (Le Hir et al., 2008a,b). Since no GCM simulation was performed above 400 PAL our CO_2 history begins at 0.12 bar.

Fig. 5 shows the atmospheric CO_2 evolution in the aftermath of snowball Earth. Four shapes of global CO_2 consumption have been used to decipher the role of weathering parameters in controlling how atmospheric CO_2 would have decreased in the snowball aftermath. Using the FOAM water volumetric content (MR/FOAM run), the continental weathering becomes less efficient due to enhanced dryness of the weathering profiles. Indeed, the hothouse climate plays an inhibiting role on weathering by dropping the soil water volumetric content below 20% which was the fixed value of the other experiments. Nevertheless, changes linked to the use of the FOAM water volumetric content remain minor. This is the result of the first order control played by the runoff on the weathering, bringing waters in contact with the minerals and transporting the weathering products. The soil water content only plays a secondary role on how long the runoff interacts with the minerals (i.e. residence time). Hence, the simulated CO_2 reductions are of the same order for the MR/FOAM run and the MR run. Larger effects are visible when changing the reactive surface (HR run) and even more when also changing the soil thickness (HR/thick run). After 1 million years, atmospheric CO_2 decreases to 100 PAL, 70 PAL and 20 PAL for MR, HR and HR/thick runs, respectively. Recovery timescales are thus dependent on the weathering profile parameters, though the HR run is probably the one better representing soil conditions that may have occurred after several million years of global glaciation. Hence, we can conclude that the recovery timescale from a snowball Earth is 1) on the order of a few million years in any case and 2) mostly dependent on the soil thickness, the reactive surface, and the runoff pattern.

5. The deglaciation and the cap dolostone deposition, a model-data discussion

Is it possible to explore the weathering rates during the melting phase itself? As discussed above, modelling the melting of a snowball Earth at very high CO_2 levels using a coupled ice-sheet — climate model remains a technical challenge for a while because of computational limitations. Our GCM cannot at present handle rapidly melting ice sheets and sea glaciers in the initial stages of the high CO_2 world. Nevertheless, guesses can be assumed regarding the continental runoff and temperature resulting from the melting phase. A

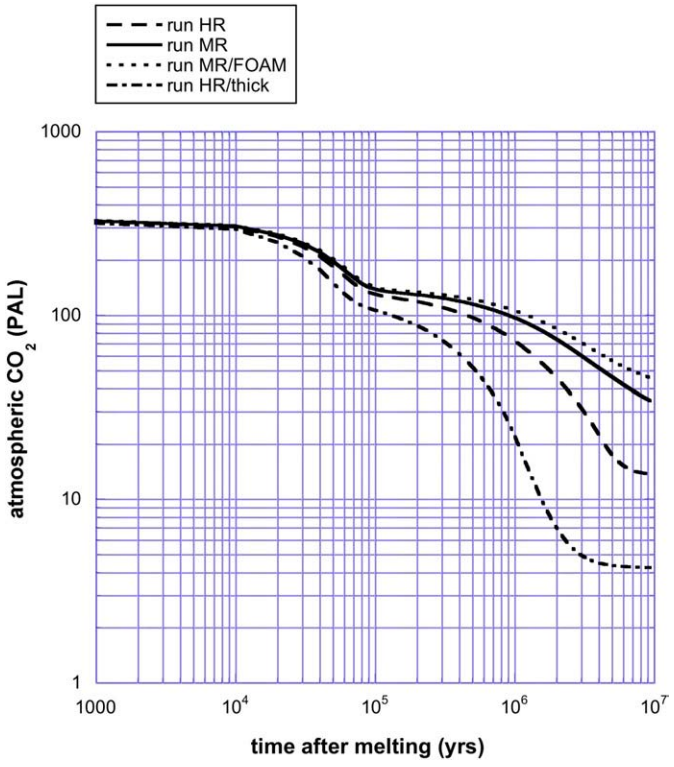

Fig. 5. Post-snowball atmospheric CO_2 evolution calculated by the simplified COMBINE geochemical module, using the weathering rates calculated by the WITCH mechanistic weathering model in the four cases described above.

Please cite this article as: Le Hir, G., et al., The snowball Earth aftermath: Exploring the limits of continental weathering processes, Earth Planet. Sci. Lett. (2008), doi:10.1016/j.epsl.2008.11.010

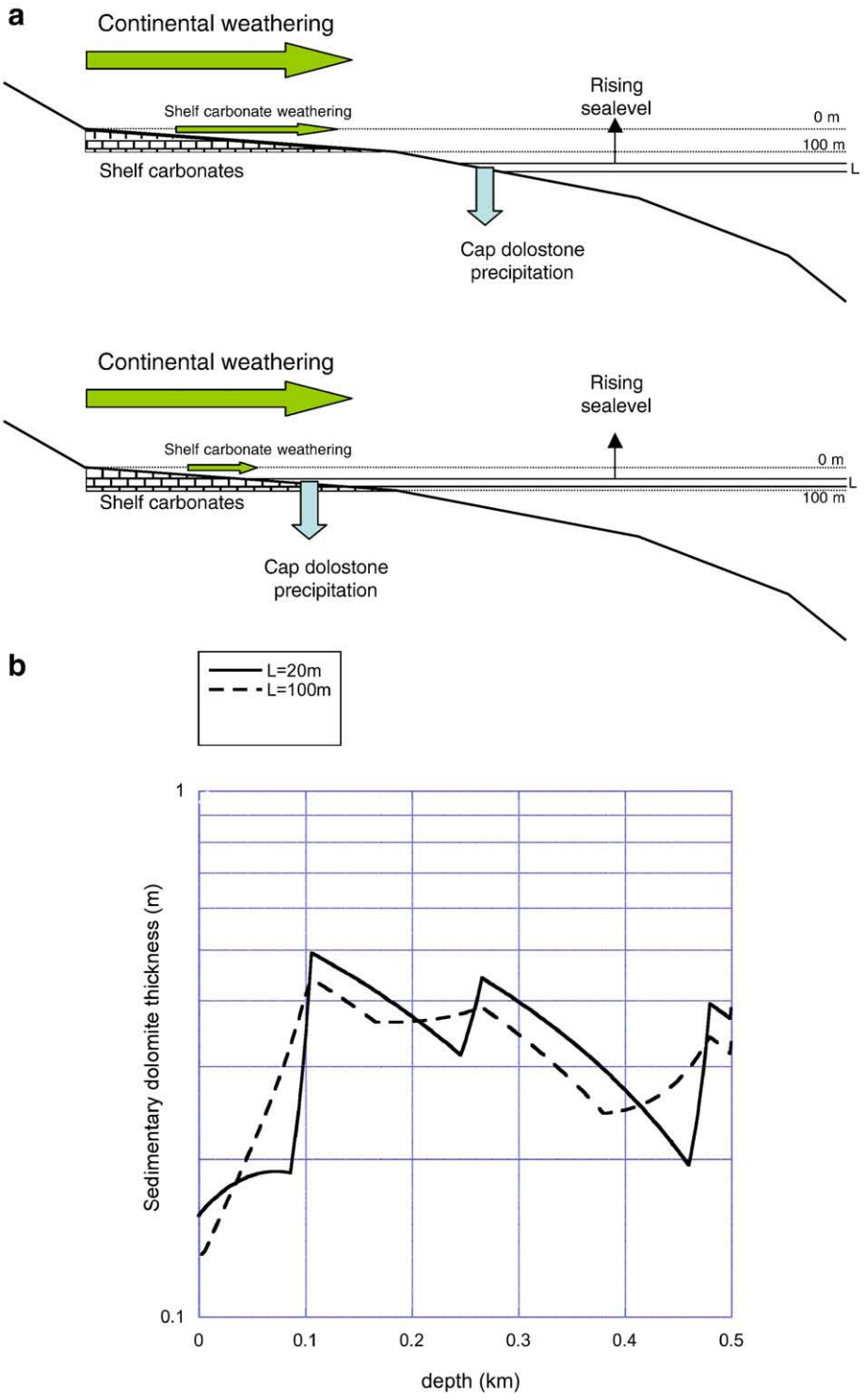

Fig. 6. a) Numerical model used to calculate the deposition rate of the cap dolostones. b) Cap dolostones thickness accumulated during the deglaciation phase (lasting 10 kyr), as a function of the level below the pre-glacial sealevel (assumed to be located at 0 m). 0.5 km represents the sea-level drop linked to Neoproterozic global glaciations. *L* denotes the thickness of the water layer intercepting the seafloor and from which cap dolostone are precipitated.

previous modelling study coupling a climate and an ice-sheet models calculates a land-ice volume reaching ~200×10^6 km^3 for a global glaciation (Donnadieu et al., 2003), a value in close agreement with a glacio-eustatic sea level fall of 500 m or more deduced from the stratigraphic record of end-Cryogenian glaciation in Namibia (Hoffman et al., 2007). If the melting spans 10 kyrs (Hoffman et al., 2007) and if the icecap melts linearly with time, this would correspond to a runoff flux of 20 cm/yr during 10 kyr. The contribution of rainfall to this runoff cannot be estimated accurately without a coupled GCM-ice sheet simulation of the melting of the snowball. This is a fruitful area for future inquiry. Indeed, during deglaciation, it is possible that precipitation was focused on low latitude continents owing to newly formed ice-free oceanic areas and to resulting steep meridional temperature gradient (Peyser and Poulsen, 2008), but this process cannot be explored here. Regarding temperature, we assume that the melt waters responsible for the dissolution of the minerals are around

Please cite this article as: Le Hir, G., et al., The snowball Earth aftermath: Exploring the limits of continental weathering processes, Earth Planet. Sci. Lett. (2008), doi:10.1016/j.epsl.2008.11.010

1 °C. At such a low temperature, the solubility of carbonate minerals increases, but silicate weathering is strongly inhibited. Atmospheric CO_2 is fixed at 400 PAL. Under such conditions (*Deglac* run), the predicted silicate weathering flux obtained by WITCH only consumes 15.11×10^{12} mol CO_2/yr despite very high CO_2 pressure acidifying the percolating solutions. This value is only slightly above the present day estimate (Gaillardet et al., 1999). The net atmospheric pCO_2 drawdown linked to silicate weathering itself is insignificant owing to the melting phase duration (10 kyr) and the high atmospheric CO_2 content. This result is in agreement with the observation that the maximum silicate weathering is reached after cap dolostone deposition, i.e. after the melting and transgressive phase, as shown by Sr and Ca isotope data (Kaseman et al., 2005; Nédélec et al., 2007; Nogueira et al., 2007).

While silicate weathering rates during the deglaciation would have been relatively low, carbonate weathering should have been much higher because the dissolution of carbonate minerals is enhanced by the low temperature. Higgins and Schrag (2003) argued that the carbonate weathering flux might be responsible for the accumulation of the 18 m-thick (on average) post-glacial cap dolostones (Hoffman et al., 2007) during the melting phase, mainly resulting from the weathering of emerged carbonate platforms and intra-cratonic carbonate outcrops. To test this hypothesis, an additional carbonate lithology is added to the model, randomly along the coast line so that the carbonate weathering can be investigated with WITCH. Indeed, given the low sea-level prior to deglaciation, large carbonate (calcite and dolomite) platforms would have been exposed to subaerial weathering. The exact location of the carbonate outcrops is not important in this numerical experiment, since global climate is assigned at a fixed value for each continental grid element (runoff=20 cm/yr, temperature=1 °C), whatever its location. Assuming that these carbonate platforms accumulate prior to the snowball Earth beneath a 100 m-thick epicontinental oceanic layer, their maximum areal extent cannot exceed 20×10^6 km^2, assuming a present day oceanic hypsometry. In addition to these emerged carbonate shelves, ancient carbonates in the continental interior would also have been subjected to weathering. Today, intra-continental carbonate outcrops cover about 20×10^6 km^2 of the land surface (Amiotte-Suchet et al., 2003). We use the same value for the Neoproterozoic continental surface. Thus, the assumed maximum carbonate surface area in the direct aftermath of the snowball (as long as sealevel is below the 100 m depth level) was 40×10^6 km^2. In our model, 50% of these outcrops are assumed to be calcite and 50% dolomite and the water draining these areas are assumed to be saturated with respect to the relevant carbonate mineral. The WITCH simulation can be performed at very high CO_2 levels. Indeed we prescribe the climate for each continental grid element (constant runoff and temperature). The FOAM GCM output are not used here and the 400 PAL threshold is not a limitation for the WITCH model. Because it has been suggested that 400 PAL might be too low (Pierrehumbert, 2004) to melt the snowball Earth, we perform our simulations assuming that the CO_2 level was around 1000 PAL, thus further maximizing the continental weathering rates and consequently the cap-carbonates deposition rate.

Since the WITCH model calculates the Mg^{2+} and Ca^{2+} flux to the ocean, we can convert these fluxes in thickness of cap dolostones being deposited, assuming that chemical conditions for cap dolostones to precipitate are satisfied (Font et al., 2006), a deposition surface and a mean density of 2600 kg/m^3 for the sedimentary carbonates. We deliberately choose this mass balance method since the kinetics of cap dolostone precipitation is not known. To be as realistic as possible, we build up a numerical model calculating the deposition surface as a function of the sealevel during the melting phase (the so-called "hypsometric model", Fig. 1). The depositional surface is estimated assuming the present day oceanic hypsometry, and that cap dolostones where deposited within a water layer of thickness L (Fig. 6a). This water layer rises from the slope along the shelf, as the oceanic volume rises linearly in response to the icecap melting, forcing sealevel to rise. The interception between the seafloor surface and this water layer defines the area of cap dolostones accumulation. All Mg^{2+} originating from continental weathering is assumed to precipitate instantaneously on this area, assuming consequently that the chemical conditions required to precipitate dolostones are satisfied within the considered water layer. We also account for the decrease in the surface of emerged carbonate platforms once the sealevel reaches 100 m below its pre-perturbation value (see Fig. 6a).

With L=20 m, we found that, if the melting phase lasts 10 kyr, a maximum of 50 cm of cap dolostones could be accumulated by using all the Mg^{2+} from coeval continental weathering (Fig. 6b). The calculated thickness of cap-carbonates is not heavily dependent on the assumed thickness L of the water layer in which cap dolostones are deposited (Fig. 7), nor on the duration of the melting phase (since a longer duration implies a lower runoff, and hence a lower weathering). The calculated thickness of the cap dolostones is about 40 times lower than the mean compiled value of 18.5 m (Hoffman et al., 2007), although this is the mean arithmetic thickness, without weighting by the original depositional area. To reconcile the model output with the data would require that the surface of dolomitic outcrop being weathered was 40 times greater than the assumed 20×10^6 km^2, which is clearly unrealistic. Conversely, if we allow that the area over which cap dolostones were precipitated was lower by a factor of 10, then cap dolostones on average 5 meters thick would have been deposited. While the base-Ediacarian cap dolostones in Namibia and Death Valley, for example, are very thick, the equivalent cap dolostones in Svalbard, East Greenland, northern Norway, Australia, and elsewhere are on average much thinner. If these thinner cap dolostones are in fact more typical and their areal extent restricted, then the carbonate weathering model for cap dolostone precipitation may in fact be valid. This also suggests that the thickness of cap dolostones was heterogeneous over continental shelves and that high average thicknesses of preserved cap dolostones are a preservational bias. In addition, as noted above, we do not take into account the runoff component resulting from the precipitation occurring during the deglaciation itself but the one resulting from the continental ice cover melting. Although an accurate estimate of the former one depends on coupled GCM ice-sheet simulations in this peculiar context, we can note that the runoff calculated by FOAM at 400 PAL saturates around 30–33 cm/yr. By adding both components (the one from the ice-sheet melting and the one from the ocean-atmosphere system), we obtain a mean thickness of 82 cm, a value which remains far for the one suggested by Hoffman et al. (Hoffman et al., 2007). Hence, even with the shortcomings of our model, our results still support the possibility that thinner cap dolostones are in fact more typical during the aftermath of the snowball Earth. This conclusion remains to be confirmed in the future.

Alternatively, the timescale for cap dolostone precipitation may be grossly underestimated. In fact, the timescale of cap dolostone precipitation is a subject of significant debate (Hoffman et al., 2007). Importantly, the stratigraphic context of the cap dolostone unambiguously constrains its timing of deposition to the period spanning the post-glacial eustatic rise in sea level. Rapid deposition of the cap dolostone (2000–10000 years; Hoffman et al., 2007) has thus been inferred based on modelled high rates of ice sheet decay at the end of the snowball (Hyde et al., 2000) and by analogy with Quaternary deglaciation (Bard et al., 1990). However, magnetostratigraphic data from multiple successions imply that cap dolostones span multiple magnetic reversal events (Trindade et al., 2003; Kilner et al., 2005), suggesting that the cap dolostones accumulated over several hundreds of thousands of years. Whether this timescale may be reconciled with the climate models is still an open question, pending on a careful modeling of the melting phase.

6. Conclusion

In this study, we force a numerical model predicting continental weathering with 3D-climate model output to investigate the climate

Please cite this article as: Le Hir, G., et al., The snowball Earth aftermath: Exploring the limits of continental weathering processes, Earth Planet. Sci. Lett. (2008), doi:10.1016/j.epsl.2008.11.010

and weathering response during the supergreenhouse climate following the snowball Earth event. The main conclusion of this study is that post-glacial silicate weathering was likely not as vigorous as commonly assumed (Higgins and Schrag, 2003; Hoffman et al., 2007). This result is largely due to the non-linear relationship between average continental temperatures and runoff rates under very high CO_2 levels. This relative dryness of the supergreenhouse climate is linked to physical constraints governing the surface energy budget. Indeed the energy released by the evaporation cannot overcome the net solar energy absorbed in surface. Since the incoming solar energy is not enhanced by increasing CO_2, the evaporation rates, and thus the intensity of the hydrological cycle, level off at high CO_2 levels. For example, even at 400 times the present CO_2 pressure, continental runoff is only 22% higher than the calculated present day values. As a consequence, under a 400 PAL CO_2 climate, our simulated discharge of dissolved elements from continental weathering into the ocean shows at best a 10-fold increase compared to the present-day estimate. As a consequence, the time required to restore CO_2 concentrations to roughly pre-glacial levels is on the order of a few million years, rather than a few thousand years, as has been previously assumed (Higgins and Schrag, 2003). Hence, an unusually warm climate may have persisted for many million years, thus extending the duration of the environmental filter on the biospheric evolution. A more protracted timescale for the recovery from the post-snowball super-greenhouse should be testable using isotopic proxies (e.g. $^{87}Sr/^{86}Sr$, $\delta^{26}Mg$) of the continental weathering.

A final important result of our linked numerical models is that, assuming a timescale of deglaciation of 10 kyr, total continental weathering (carbonate+silicate) supplies only enough Mg^{2+} to accumulate a maximum of 50 cm of cap dolostone over the continental shelves, which is over an order of magnitude lower than the calculate average global thickness of base-Ediacaran cap dolostones (Hoffman et al., 2007). Our history of continental rock dissolution in the aftermath of the snowball glaciation is also in agreement with the isotopic proxies for continental weathering that suggest that the major increase in silicate weathering occurred directly after cap dolostone deposition (Kaseman et al., 2005).

Acknowledgments

This study was funded by the French National Agency for Research program ANR-06-BLAN-0347 and by the CNRS/INSU through the ECLIPSE program. We thank Praksys for the maintenance of the cluster of PC at the LMTG (www.praksys.org). We thank Lee Kump and an anonymous referee for their insightful reviews, and Peter deMenocal for the quality of the editorial procedure.

References

Allen, M.R., Ingram, J., 2002. Constraints on future changes in climate and the hydrologic cycle. Nature 419, 224–232.
Amiotte-Suchet, P., Probst, J.L., Ludwig, W., 2003. World wide distribution of continental rock lithology: implications for atmospheric/soil CO_2 uptake by continental weathering and alkalinity river transport to the oceans. Glob. Biogeochem. Cycles 17, doi:10.1029/2002GB001891.
Bao, H.M., Lyons, J.R., Zhou, C., 2008. Triple oxygen isotope evidence for elevated CO_2 levels after a Neoproterozoic glaciation. Nature 453, 504–506.
Bard, E., Hamelin, B., Fairbanks, R.G., Zindler, A., 1990. Calibration of the ^{14}C timescale over the past 30.000 years using mass spectrometric U–Th ages from Barbados corals. Nature 345, 405–410.
Berner, R.A., 2004. The Phanerozoic Carbon Cycle. Oxford University Press, New York. 150 pp.
Berner, E.K., Berner, R.A., 1987. The global water cycle: geochemistry and environment. Prentice Hall. 397 pp.
Brady, P.V., 1991. The effect of silicate weathering on global temperature and atmospheric CO_2. J. Geophys. Res. 96, 18101–18106.
Brunauer, S., Emmett, P.H., Teller, E., 1938. Adsorption of gases in multimolecular layers. J. Am. Chem. Soc. 60, 309–319.
Caldeira, K., Kasting, J.F., 1992. Susceptibility of the early Earth to irreversible glaciation caused by carbon dioxide clouds. Nature 359, 226–228.
Cogné, J.P., Humler, E., 2004. Temporal variation of oceanic spreading and crustal production rates during the last 180 My. Earth Planet. Sci. Lett. 227, 427–439.
Condon, D., Zhu, M.Y., Bowring, S., Wang, W., Yang, A.H., Jin, Y.G., 2005. U–Pb ages from the Neoproterozoic Doushantuo Formation, China. Science 308, 95–98.
Dessert, C., Dupré, B., François, L.M., Schott, J., Gaillardet, J., Chakrapani, G.J., Bajpai, S., 2001. Erosion of Deccan Traps determined by river geochemistry: impact on the global climate and the $^{87}Sr/^{86}Sr$ ratio o.f seawater. Earth Planet. Sci. Lett. 188, 459–474.
Devidal, J.L., Schott, J., Dandurand, J.L., 1997. An experimental study of kaolinite dissolution and precipitation kinetics as a function of chemical affinity and solution composition at 150 °C, 40 bars, and pH 2, 6.8, and 7.8. Geochim. Cosmochim. Acta 61, 5165–5186.
Donnadieu, Y., Fluteau, F., Ramstein, G., Ritz, C., Besse, J., 2003. Is there a conflict between the Neoproterozoic glacial deposits and the snowball Earth interpretation: an improved understanding with numerical modeling. Earth Planet. Sci. Lett. 208, 101–112.
Donnadieu, Y., Pierrehumbert, R.T., Fluteau, F., Jacob, R., 2006. Modelling the primary control of paleogeography on Cretaceous climate. Earth Planet. Sci. Lett. 248, 426–437.
Drever, J.I., 1997. The geochemistry of natural waters. Prentice Hall, Upper Saddle River, New Jersey 07458. 436 pp.
Eyring, H., 1935. The activated complex in chemical reactions. J. Chem. Phys. 3, 107–115.
Font, E., Nédélec, A., Trindade, R., Macouin, M., Charrière, A., 2006. Chemostratigraphy of the Neoproterozoic Mirassol d'Oeste cap dolostones (Mato Grosso, Brazil): a model for Marinoan cap dolostone formation. Earth Planet. Sci. Lett. 250, 89–103.
Gaffin, S., 1987. Ridge volume dependence on seafloor generation rate and inversion using long term sealevel change. Am. J. Sci. 287, 596–611.
Gaillardet, J., Dupré, B., Louvat, P., Allègre, C.J., 1999. Global silicate weathering and CO_2 consumption rates deduced from the chemistry of the large rivers. Chem. Geol. 159, 3–30.
Goddéris, Y., Joachimski, M.M., 2004. Global change in the late Devonian: modelling the Frasnian–Famennian short-term carbon isotope excursions. Palaeogeogr. Palaeoclimatol. Palaeoecol. 202, 309–329.
Goddéris, Y., Nédelec, A., Donnadieu, Y., Dupré, B., Dessert, C., François, L.M., Grard, A., Ramstein, G., 2003. The Sturtian glaciation: Fire and ice. Earth Planet. Sci. Lett. 211, 1–12.
Goddéris, Y., François, L.M., Probst, A., Schott, J., Moncoulon, D., Labat, D., Viville, D., 2006. Modelling weathering processes at the catchment scale with the WITCH numerical model. Geochim. Cosmochim. Acta 70, 1128–1147.
Gough, D.O., 1981. Solar interior structure and luminosity variations. Sol. Phys. 74, 21–34.
Held, I.M., Soden, B.J., 2006. Robust responses of the hydrological cycle to global warming. J. Clim. 19, 5686–5699.
Higgins, J.A., Schrag, D.P., 2003. Aftermath of a snowball Earth. Geochem. Geophys. Geosyst. 4, doi:10.1029/2002GC000403.
Hoffman, P.F., Kaufman, A.J., Halverson, G.P., Schrag, D.P., 1998. A Neoproterozoic Snowball Earth. Science 281, 1342–1346.
Hoffman, P.F., Halverson, G.P., Schrag, D.P., 2004. On the consistent sequence of mineralogy and bedforms in post-glacial cap carbonates of Marinoan (ca 635 Ma) age on different paleomargins: steady-state ocean stratification during a post-snowball Earth marine transgression ? Annual Geological Society of America Annual meeting, Denver.
Hoffman, P.F., Halverson, G.P., Domack, E.W., Husson, J.M., Higgins, J.A., Schrag, D.P., 2007. Are basal Ediacaran (635 Ma) post-glacial "cap-dolostones" diachronous ? Earth Planet. Sci. Lett. 258, 114–131.
Holland, H.D., 1978. The chemistry of Oceans and Atmosphere. Wiley, New York. 351 pp.
Hyde, W.T., Crowley, T.J., Baum, S.K., Peltier, W.R., 2000. Neoproterozoic "snowball Earth" simulations with a coupled climate/ice sheet model. Nature 405, 425–429.
Jacob, R., 1997. Low frequency variability in a simulated atmosphere ocean system. Univ. Wisconsin-Madison.
Kahle, M., Kieber, M., Reinhold, J., 2002. Carbon storage in loess derived surface soils from Central Germany: influence of mineral phase variables. J. Plant. Nutr. Soil Sci. 165, 141–149.
Kaseman, S.A., Hawkesworth, C.J., Prave, A.R., Fallick, A.E., Pearson, P.N., 2005. Boron and calcium isotope composition in Neoproterozoic carbonate rocks from Namibia: evidence for extreme environmental change. Earth Planet. Sci. Lett. 231, 73–86.
Kilner, B., MacNiocaill, C., Brasier, M., 2005. Low-latitude glaciation in the Neoproterozoic of Oman. Geology 33, 413–416.
Le Hir, G., Goddéris, Y., Donnadieu, Y., Ramstein, G., 2008a. A geochemical modelling study of the evolution of the chemical composition of seawater linked to a snowball glaciation. Biogeosciences 5, 253–267.
Le Hir, G., Goddéris, Y., Ramstein, G., Donnadieu, Y., 2008b. A scenario for the evolution of the atmospheric pCO_2 during a snowball Earth. Geology 36, 47–50.
Meert, J.G., Torsvik, T.H., 2003. The making and unmaking of a supercontinent: Rodinia revisited. Tectonophysics 375, 261–288.
Nédélec, A., Affaton, P., France-Lanord, C., Charrière, A., Alvaro, J.J., 2007. Sedimentology and chemostratigraphy of the Bwipe Neoproterozoic cap carbonates (Ghana, Volta Basin): a record of microbial activity in a peritidal environment. C. R. Geosci. 339, 516–518.
Nogueira, A.C.R., Riccomini, C., Sial, A.N., Moura, C.A.V., Trindade, R., Fairchild, T.R., 2007. Carbon and strontium isotope fluctuations and paleoceanographic changes in the late Neoproterozoic Araras carbonate platform, southern Amazon craton, Brazil. Chem. Geol. 237, 168–190.
Oelkers, E.H., Schott, J., Devidal, J.L., 1994. The effect of aluminum, pH and chemical affinity on the rates of aluminosilicate dissolution reactions. Geochim. Cosmochim. Acta 58, 2011–2024.
Oliva, P., Viers, J., Dupré, B., 2003. Chemical weathering in granitic crystalline environments. Chem. Geol. 202, 225–256.

Please cite this article as: Le Hir, G., et al., The snowball Earth aftermath: Exploring the limits of continental weathering processes, Earth Planet. Sci. Lett. (2008), doi:10.1016/j.epsl.2008.11.010

Peyser, C.E., Poulsen, C.J., 2008. Controls on Permo-Carboniferous precipitation over tropical Pangaea: a GCM sensitivity study. Palaeogeogr. Palaeoclimatol. Palaeoecol. 268, 181–192.
Pierrehumbert, R.T., 1999. Subtropical water vapor as a mediator of rapid global climate change. In: Clarks, P.U., Webb, R.S., Keigwin, L.D. (Eds.), Mechanisms of global change at the Millenial time scales. Geophys. Monogr. Ser., vol. 112. American Geophysical Union, Washington D.C., p. 394.
Pierrehumbert, R.T., 2002. The hydrologic cycle in deep-time climate problems. Nature 419, 191–198.
Pierrehumbert, R.T., 2004. High levels of atmospheric carbon dioxyde necessary for the termination of global glaciation. Nature 429, 646–649.
Poulsen, C.J., 2003. Absence of a runaway ice-albedo feedback in the Neoproterozoic. Geology 31, 115–118.
Poulsen, C.J., Jacob, R.L., 2004. Factors that inhibit snowball Earth simulation. Paleoceanography 19, doi:10.1029/2004PA001056.
Rapp, A.D., Kummerow, C., Berg, W., Griffith, B., 2005. An evaluation of the proposed mechanism of the adaptative infrared iris hypothesis using TRMM VIRS and PR measurements. J. Clim. 18, 4185–4194.
Rowley, D.B., 2002. Rate of plate creation and destruction: 180 Ma to present. Geol. Soc. Am. Bull. 114, 927–933.
Schott, J., Oelkers, E.H., 1995. Dissolution and crystallization rates of silicate minerals as a function of chemical affinity. Appl. Chem. 67, 903–910.
Sverdrup, H., Warfinge, P., 1995. Estimating field weathering rates using laboratory kinetics. Rev. Mineral. 31, 485–541.
Trindade, R.I.F., Font, E., D'Agrella-Filho, M.S., Nogueira, A.C.R., Riccomini, C., 2003. Low-latitude and multiple geomagnetic reversals in the Neoproterozoic Puga cap carbonate, Amazon craton. Terra Nova 15, 441–446.
Vecchi, G.A., Soden, B.J., Wittenberg, A.T., Held, I.M., Leetma, A., Harrison, M.J., 2006. Weakening of tropical Pacific atmospheric circulation due to anthropogenic forcing. Nature 441, 73–76.
Walker, J.C.G., Hays, P.B., Kasting, J.F., 1981. A negative feedback mechanism for the long-term stabilization of Earth's surface temperature. J. Geophys. Res. 86, 9776–9782.
White, A.F., Blum, A.E., 1995. Effects of climate on chemical weathering in watersheds. Geochim. Cosmochim. Acta 59, 1729–1747.

Please cite this article as: Le Hir, G., et al., The snowball Earth aftermath: Exploring the limits of continental weathering processes, Earth Planet. Sci. Lett. (2008), doi:10.1016/j.epsl.2008.11.010